Paper No. 213, Bull. ISET, Vol. 18 No. 2, June 1981, pp. 88-100

A NOTE ON THE VIBRATIONS OF A SEMI-CIRCULAR CANAL EXCITED BY PLANE SH-WAVE

NASSER MOEEN-VAZIRI* AND MIHAILO D. TRIFUNAC*

Introduction

In this paper, the problem of scattering and diffraction of plane SH waves by a semi-cylindrical canal has been investigated. This type of problem is of practical interest, for example, in the analysis and design of reinforced concrete canals. Related to this problem, there have been studies previously on: (1) the displacement around a semi-cylindrical canyon in an elastic half-space (Trifunac, 1973); (2) the interaction of a shear wall with the soil for incident plane SH waves (Trifunac, 1972); and (3) surface motion of a semi-cylindrical alluvial valley for incident plane SH waves (Trifunac, 1971).

The geometrical simplicity of the model studied here limits the practical applicability of the results presented here for engineering design of actual canals. However, the exact nature of the present solution offers the possibility for testing other approximate methods. It also enables one to investigate the significance of various physical parameters governing this problem in a continuous and explicit manner.

The Model

The cross-section of the two-dimensional model studied in this paper is shown in Figure 1. It represents a half-space ($y>0$) in which a semi-cylindrical canal with inner radius b and outer radius a is situated. The material properties of the elastic, isotropic and homogeneous half-space are characterized by the rigidity, μ_1, and velocity of shear waves, β_1, while those of the canal wall are μ_2 and β_2.

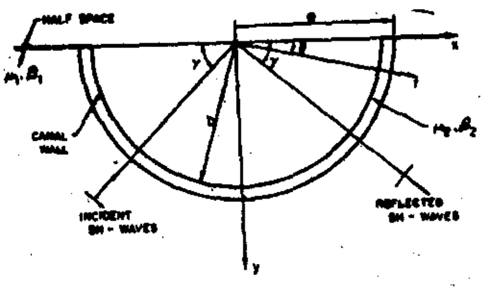

Figure 1 Semi-Cylindrical Canal and the Surrounding Half-Space

*School of Engineering, Department of Civil Engineering, University of Southern California, University Park, Los Angeles, California 90007, U.S.A.

Two coordinate systems are employed. The rectangular coordinate system is centered in the axis of the cylinder with positive x pointing to the right, and positive y pointing down. The cylindrical coordinate system, consisting of the radial distance r and the angle θ, measured from the positive x-coordinate, has a common origin with the rectangular system.

Excitation and Solution of the Problem

The excitation of the half half-space, u_z, is assumed to consist of an infinite train of plane SH waves with frequency ω and particle motion in the z-direction as follows

$$u_z^i = \exp i\omega\left(t - \frac{x}{c_x} + \frac{y}{c_y}\right) \tag{1}$$

For an incident angle γ, the phase velocities along the x-axis c_x and y-axis c_y are given by

$$c_x = \frac{\beta}{\cos\gamma} \tag{2}$$

$$c_y = \frac{\beta}{\sin\gamma}. \tag{3}$$

In the absence of a canal, the incident motion would reflect from the plane free surface ($y=0$), and incident waves u_z^i and reflected waves u_z^r would interfere to give the resulting motion of half-space

$$u_z^i + u_z^r = 2\exp\left[i\omega\left(t - \frac{x}{c_x}\right)\right]\cos\left(\frac{\omega y}{c_y}\right) \tag{4}$$

In the present problem, for large x, where the effects of the waves scattered from and diffracted around the canal become very small, equation (4) represents the actual half-space motion.

Close to the canal, incident and reflected waves u_z^i and u_z^r are scattered and diffracted by the outer surface of the canal. This new group of scattered and diffracted waves is called u_z^R. Wave energy is also refracted into the the lining of the canal. This motion is denoted by u_z^f. The total displacement field, u_z^t, resulting from the incident plane SH waves, u_z^i, represents a superposition of u_z^i, u_z^r and u_z^R waves. This total displacement field can be written as follows

$$u_z^t = u_z^i + u_z^r + u_z^R \tag{5}$$

For a canal of semi-cylindrical shape, the cylindrical system is suitable for use, since the boundary conditions along the inner and outer surface of the canal are then significantly simplified. It is therefore convenient to represent both the excitation [equation (4)] and the scattered and diffracted waves u_z^R in terms of functions of r and θ. It can be shown that with

$$x = r\cos\theta, \quad y = r\sin\theta$$

$$u_z^i = \exp i\left[\omega t - k_\beta r\cos(\theta+\gamma)\right]. \tag{6}$$

It follows then that

$$u_z^i + u_z^r = 2\sum_{n=0}^{\infty} \varepsilon_n (-i)^n J_n(k_1 r)\cos n\theta\cos n\gamma \tag{7}$$

where $J_p(x)$ are Bessel functions of the first kind with argument x and order p, and $k_1=\omega/\beta_1$ is a wave number in the half-space. The coefficient d_n is defined as follows

$$d_n=\begin{cases}1 & \text{for } n=0\\ 2 & \text{for } n=1\end{cases}$$

Solution of the Problem

Both the total displacement field, u_z^t, and refracted waves, u_z^f, must satisfy the differential equation

$$\frac{\partial^2 u_z}{\partial r^2}+\frac{1}{r}\frac{\partial u_z}{\partial r}+\frac{1}{r^2}\frac{\partial^2 u_z}{\partial \theta^2}=\frac{1}{\beta^2}\frac{\partial^2 u_z}{\partial t^2} \tag{8}$$

where $u_z=u_z^t$, $\beta=\beta_1$ in the elastic half-space, and

$u_z=u_z^f$, $\beta=\beta_2$ in the elastic lining of the canal wall.

The boundary conditions are (assuming welded contact between the half-space and the canal)

$$(\sigma_{\theta z})_1=\frac{\mu_1}{r}\frac{\partial u_z^t}{\partial \theta}=0 \qquad \text{at} \quad \theta=0 \text{ and } \theta=\pi,\ r>a \tag{9}$$

$$(\sigma_{\theta z})_2=\frac{\mu_2}{r}\frac{\partial u_z^f}{\partial \theta}=0 \qquad \text{at} \quad \theta=0 \text{ and } \theta=\pi,\ b<r<a \tag{10}$$

$$u_z^t=u_z^f \qquad \text{at} \quad r=a \text{ and } 0\leqslant\theta\leqslant\pi \tag{11}$$

$$\mu_1\frac{\partial u_z^t}{\partial r}=\mu_2\frac{\partial u_z^f}{\partial r} \qquad \text{at} \quad r=a \text{ and } 0<\theta<\pi \tag{12}$$

$$(\sigma_{rz})_2=\mu_2\frac{\partial u_z^f}{\partial r}=0 \qquad \text{at} \quad r=b \text{ and } 0<\theta<\pi \tag{13}$$

The wave u_z^R represents an outgoing wave, since it consists of waves scattered from and diffracted around the semi-cylindrical canal. It must satisfy the differential equation (8) and the stress-free boundary condition equation (9). The sum $u_z^t=u_z^i+u_z^r+u_z^R$ must also satisfy the boundary condition equations (11) and (12). The wave u_z^R satisfying equations (8) and (9) can be written as

$$u_z^R=\sum_{n=0}^{\infty} a_n H_n^{(2)}(k_1 r)\cos n\theta, \quad k_1=\frac{\omega}{\beta_1} \tag{14}$$

where $H_p^{(2)}(x)$ is the Hankel function of the second kind with argument x and order p. The wave u_z^f represents an outgoing and incoming wave, since it consists of waves refracted into the lining of the canal wall. It must satisfy the differential equation (8) and the stress-free boundary condition equations (10) and (13). It must also satisfy the boundary condition equations (11) and (12). The wave u_z^f can be written as

$$u_z^f=\sum_{n=0}^{\infty}[b_n H_n^{(1)}(k_2 r)+c_n H_n^{(2)}(k_2 r)]\cos n\theta,\ k_2=\frac{\omega}{\beta_2} \tag{15}$$

where $H_p^{(1)}(x)$ is the Hankel function of the first kind with argument x and order p. The constants b_n and c_n are complex constants and are determined along with constant a_n by making use of the boundary conditions. They are given as, for $n=0, 1, 2, \ldots$

$$a_n = -2d_n(-i)^n \cos n\gamma \frac{\left[J_{n-1}(k_1a)-\frac{n}{k_1a}J_n(k_1a)\right]P_n(k_2a)-\frac{\mu_2}{\mu_1}\frac{k_2}{k_1}J_n(k_1a)Q_n(k_2a)}{\left[H^{(1)}_{n-1}(k_1a)-\frac{n}{k_1a}H^{(1)}_n(k_1a)\right]P_n(k_2a)-\frac{\mu_2}{\mu_1}\frac{k_2}{k_1}H^{(1)}_n(k_1a)Q_n(k_2a)} \tag{16}$$

$$c_n = -2d_n(-i)^n \cos n\gamma \frac{J_{n-1}(k_1a)H^{(1)}_n(k_1a)-J_n(k_1a)H^{(1)}_{n-1}(k_1a)}{\left[H^{(1)}_{n-1}(k_1a)-\frac{n}{k_1a}H^{(1)}_n(k_1a)\right]P_n(k_2a)-\frac{\mu_2}{\mu_1}\frac{k_2}{k_1}H^{(1)}_n(k_1a)Q_n(k_2a)} \tag{17}$$

$$b_n = -G_n(k_2b)\, c_n$$

where $\quad P_n(k_2a)=H^{(1)}_n(k_2a)-G_n(k_2b)H^{(2)}_n(k_2a)$

$$Q_n(k_2a)=H^{(1)}_{n-1}(k_2a)-\frac{n}{k_2a}H^{(1)}_n(k_2a)-G_n(k_2b)\left[H^{(2)}_{n-1}(k_2a)-\frac{n}{k_2a}H^{(2)}_n(k_2a)\right]$$

$$G_n(k_2b)=\frac{k_2bH^{(1)}_{n-1}(k_2b)-nH^{(1)}_n(k_2b)}{k_2bH^{(2)}_{n-1}(k_2b)-nH^{(2)}_n(k_2b)}$$

Once a_n, b_n and c_n are determined, the total solution $u_z^i+u_z^r+u_z^s$ is defined everywhere for $r>a$ and $0\leqslant\theta\leqslant\pi$, and also the refracted waves u_z^f are defined in the canal wall.

For the case $\mu_2=0$, the case of a semi-cylindrical canyon of radius a in an elastic half-space equation (16) reduces to the equation for the case of a semi-cylindrical canyon derived in [1].

For the case $\mu_2\rightarrow\infty$, the case of a semi-cylindrical canal with rigid wall, equation (16) in limit reduces to the equation for a rigid semi-cylindrical foundation without any elastic shear wall erected on the foundation as derived in [2] with $M_b=0$ (where M_b represents the mass per unit length of the building erected on rigid foundation.

For the case $b\rightarrow 0$, the case of a semi-cylindrical alluvial valley, equation (16), reduces to the equation for the case of semi-cylindrical alluvial valley as derived in [3].

Surface Displacement and Stress Amplitudes

For the seismological and earthquake engineering applications, a useful aspect of the above analysis is the description of the displacement and stress amplitudes along the surface of the half-space near the canal and on the surface of the canal itself.

For the plane SH wave excitation with amplitude 1, the resulting motion can be characterized by the modulus, of displacement amplitude:

$$\text{displ. amplitude} \equiv |u_z| \equiv \{[R_e(u_z)]^2+[I_m(u_z)]^2\}^{1/2} \tag{18}$$

In the absence of the canal, the modulus of ground displacement in uniform half-space is equal to 2. In the presence of the canal, waves are scattered and diffracted along the canal, and the resulting modulus may differ from 2. Similarly, the stress, σ_{rz}, on the surface of the canal can be characterized by the normalised stress amplitude, σ^*, given by :

$$\sigma^* = \frac{\mu_1 \left. \frac{\partial u_z^t}{\partial r} \right|_{r=a}}{\mu_1 k} = \frac{\mu_2 \left. \frac{\partial u_z^f}{\partial r} \right|_{r=a}}{\mu_1 k} \tag{19}$$

where $\mu_1 k = \mu_1 \omega/\beta_1 = \mu_1 \mid \partial u_z^i/\partial r \mid$ corresponds to the stress amplitudes of the input SH wave.

Both quantities in equations (18) and (19) depend on the angle of incidence of SH waves and their frequency ω, on the shear wave velocity in the half-space and canal wall, on the inner radius and outer radius of the canal and the rigidity of the half-space and canal wall. Three of these parameters can be combined in one parameter $k_1 a$ given by

$$k_1 a = \frac{\omega a}{\beta_1} \tag{20}$$

which is also equal to

$$k_1 a = \frac{2\pi a}{\lambda_1} \tag{21}$$

and $\lambda_1 = \beta_1 T$ is the wavelength of incident waves with $T = 2\pi/\omega$. Defining another dimensionless parameter

$$\eta = \frac{2a}{\lambda_1} \tag{22}$$

$k_1 a$ becomes $\pi\eta$. As seen from equation (22), η is the ratio of the outer radius of the canal and the half-wavelength of incident waves, but it can also be thought of as the dimensionless frequency. Since $\eta = \omega a/\pi\beta_1$, it represents a dimensionless wave number, since $\eta = k_1 a/\pi$.

Discussion of Results

Figures 2 and 3 present examples of displacement amplitudes plotted versus x/a on the outer surface of the canal (r=a) and for η varying from 0.25 to 2.0, b/a=.9, $\mu_2/\mu_1 = 1/3$ and 3.0, and $k_2/k_1 = 1.5$ and 0.8. These examples correspond to a canal of rigidity which is 1/3 and 3 times the rigidity of the surrounding elastic half-space. For vertical incidence of SH waves ($\gamma = 90°$) surface displacement amplitudes are symmetric with respect to x/a=0. As γ decreases towards 0° the complexity of motion increases more for x/a < 0 than for x/a > 0 because of the interference of incident and the waves scattered from the canal. The displacement amplitudes in these figures oscillate about the mean level equal to 2. The shadow zone behind the canal is observed, e.g., for $\gamma = 60°$, $\eta = 1.0$ and $\mu_2/\mu_1 = 1/3$. For $\mu_2/\mu_1 = 3.0$, the rigid canal is more efficient in transmitting the incident wave energy to medium behind the canal. Consequently, this shadow zone almost disappears for $\mu_2/\mu_1 = 3.0$ in Figure 3.

Figures 4 and 5 present the corresponding examples, but for b/a=0.7, i.e., a canal with a thicker wall. The shadow zone for $\eta = 1.0$ and $\gamma = 60°$ now becomes more prominent for $\mu_2/\mu_1 = 1/3$. However, for $\mu_2/\mu_1 = 3.0$, as in the above example, the stiff canal, Figure 5, almost eliminates this shadow zone. For larger values of η (shorter incident waves) and for

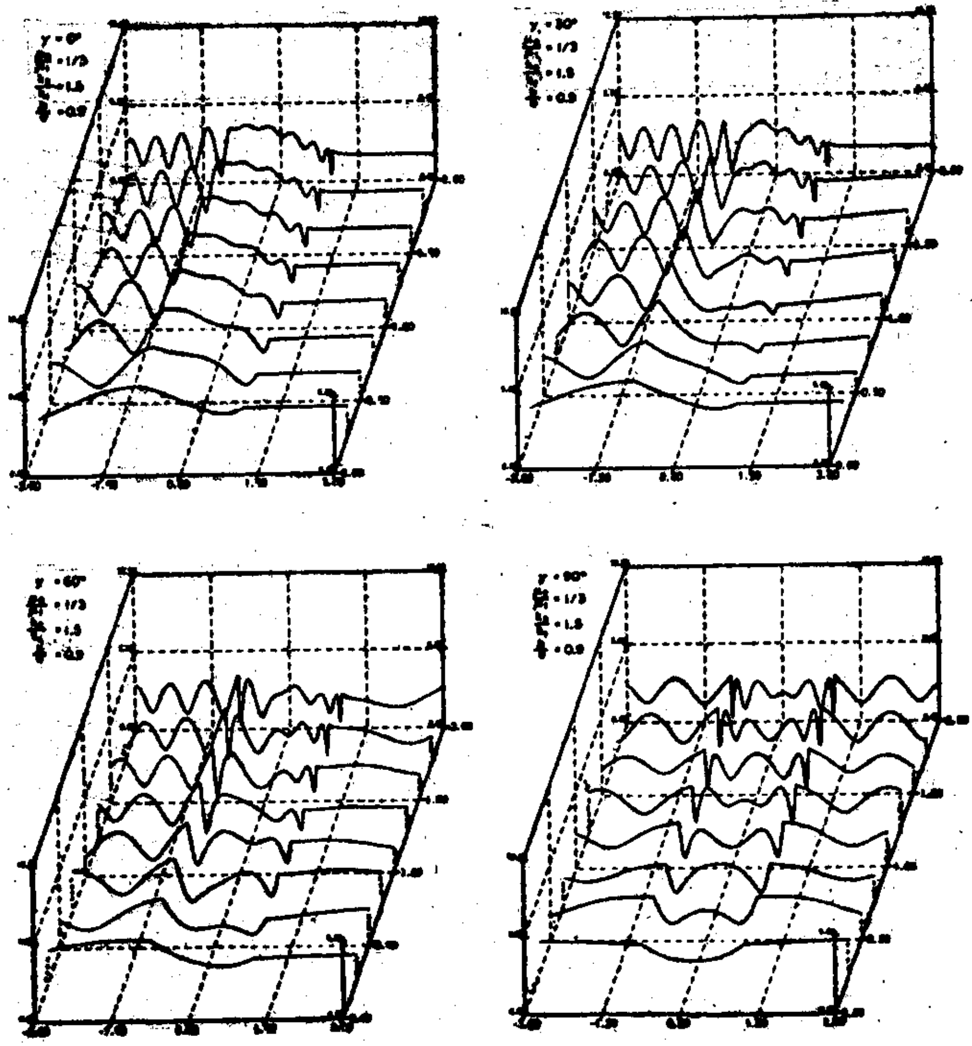

Figure 2 Surface Displacement Amplitudes for Incident SH Waves ($\gamma=90°$, $60°$, $30°$, $0°$ and $\mu_2/\mu_1=1/3$, $k_2/k_1=1.5$, $b/a=0.9$)

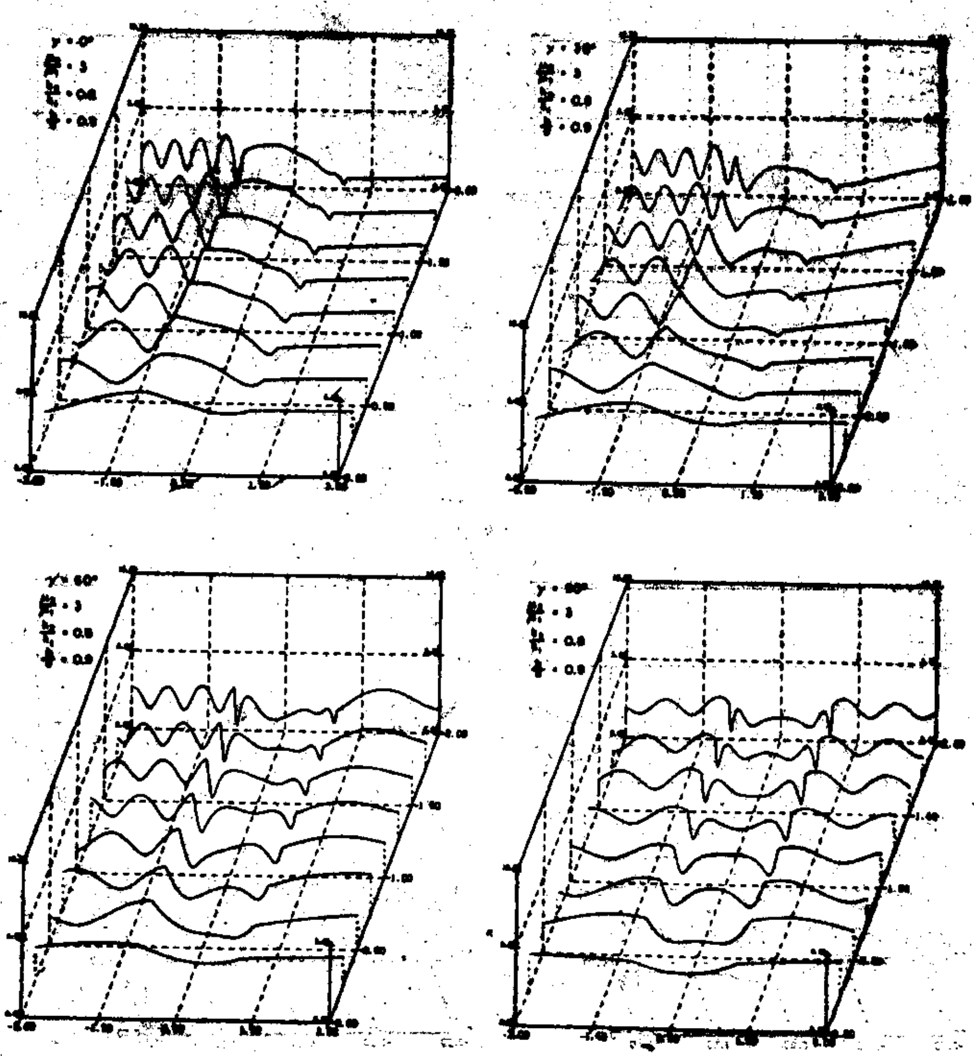

Figure 3 Surface Displacement Amplitudes for Incident Sh Waves
($\gamma = 90°, 60°, 30°, 0°$ and $\mu_2/\mu_1 = 3$, $k_2/k_1 = 0.8$, $b/a = 0.9$)

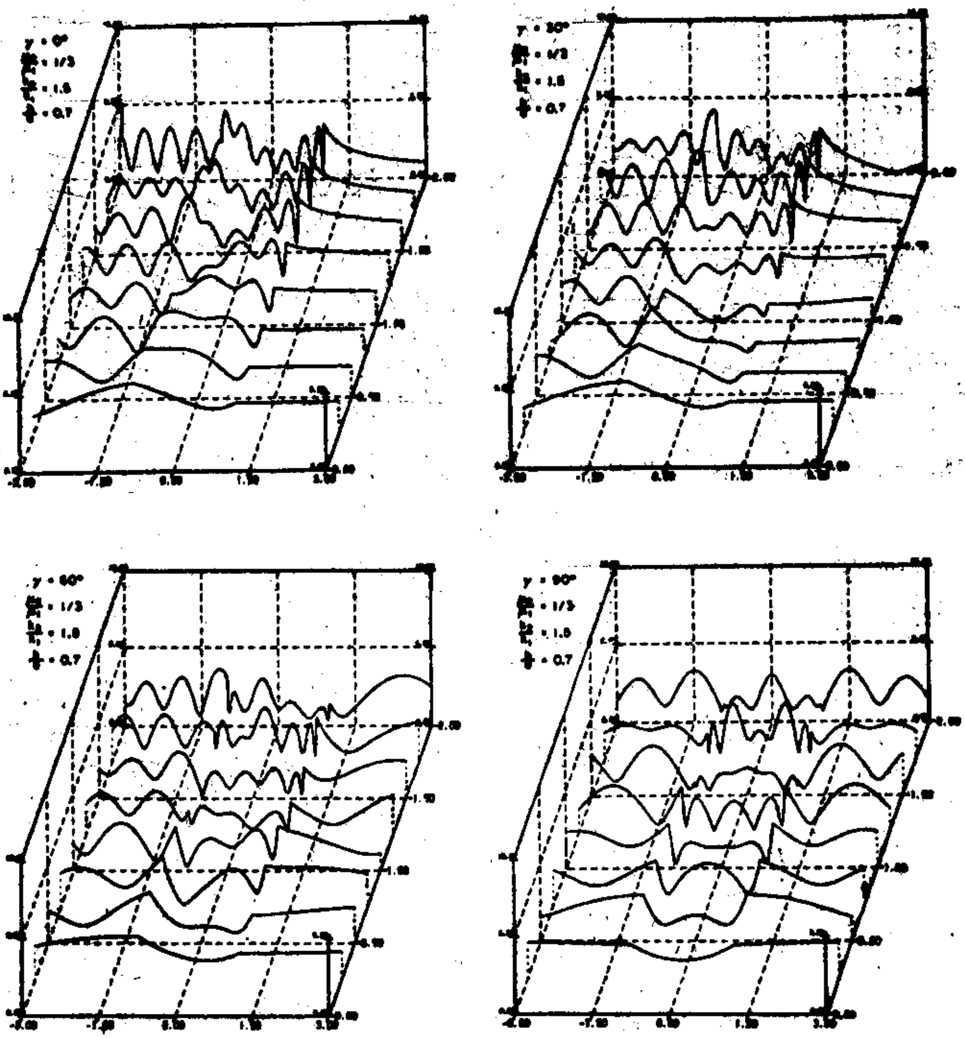

Figure 4 Surface Displacement Amplitudes for Incident SH Waves ($\gamma = 90°$, $60°$, $30°$, $0°$ and $\mu_2/\mu_1 = 1/3$, $k_2/k_1 = 1.5$, $b/a = 0.7$)

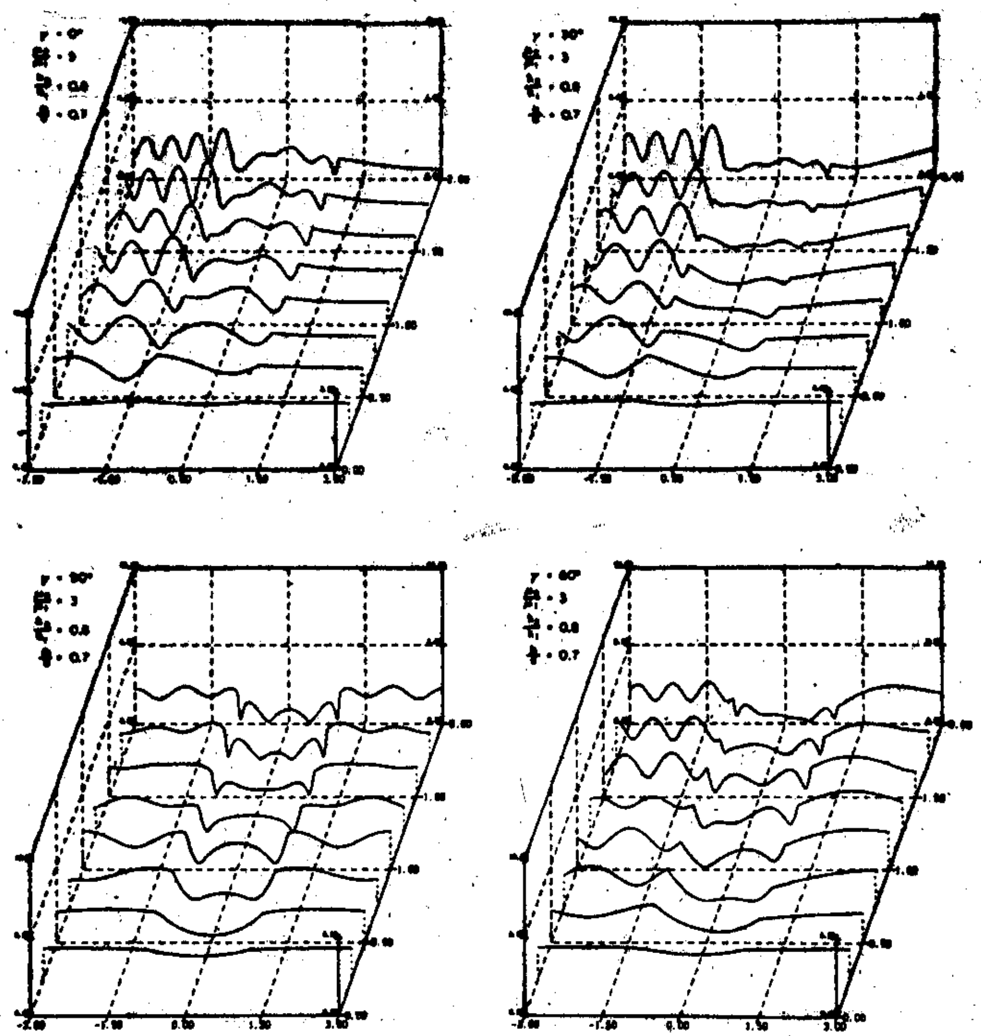

Figure 5 Surface Displacement Amplitudes for Incident SH Waves
($\gamma=90°$, $60°$, $30°$, $0°$ and $\mu_2/\mu_1=3$, $k_2/k_1=1.5$, $b/a=0.7$)

smaller γ (near 0°) the complexity of interference patterns in Figures 4 and 5 increases relative to the corresponding examples in Figures 2 and 3.

Figures 6 and 7 present the changes of normalized stress amplitudes with respect to θ, for b/a=.9, $\mu_2/\mu_1=1/3$, and 3, for $\eta=0.5$, 1, 1.5 and 2.0. It is seen that the more flexible canal is subjected to smaller stresses than the more rigid canal (Figure 7) for $\mu_2/\mu_1=3.0$.

References

1. Trifunac, M.D., "Scattering of Plane SH-Waves by a Semi-Cylindrical Canyon," Earthquake Eng. and Struc. Dyn., Vol. 1, 267-281 (1973).

2. Trifunac, M.D., "Interaction of Shear Wall with the Soil for Incident Plane SH-Waves," Bull. Seism. Soc. Amer., Vol. 62, No. 1, 63-83 (1972).

3. Trifunac, M.D., "Surface Motion of a Semi-Cylindrical Alluvial Valley for Incident Plane SH-Waves," Bull. Seism. Soc. Amer., Vol. 61, No. 6, 1755-1770 (1971).

4. Morse, P.M., and H. Feshback, *Methods of Theoretical Physics*, McGraw-Hill, New York (1953).

5. Watson, G.N., The Theory of Bessel Functions, A Treatise, University Press, Cambridge (1966).

Nomenclature

a, b	Outer and inner radii of the canal
a_n, b_n, c_n	Complex constants
$H_p^{(1)}(\cdot)$, $H_p^{(2)}(\cdot)$	Hankel functions of the of the first and second kind and of order p
i	$\sqrt{-1}$, imaginary unit
$J_p(\cdot)$	Bessel functions of the first kind and of order p
k_1	Wave number in soil, $k_1=\omega/\beta_1$
k_2	Wave number in canal, $k_2=\omega/\beta_2$
r	Radial distance in polar cordinates
u_z^i, u_z^r	Displacements due to incident and reflected SH waves
u_z^R	Displacement due to scattered SH waves
u_z^t	Resultant total displacement in the soil
u_z^f	Displacement in the canal's lining
(x, y)	Cartesian coordinate system
β_1	Shear wave velocity in the soil
β_2	Shear wave velocity in the canal
γ	Angle of incidence of SH waves

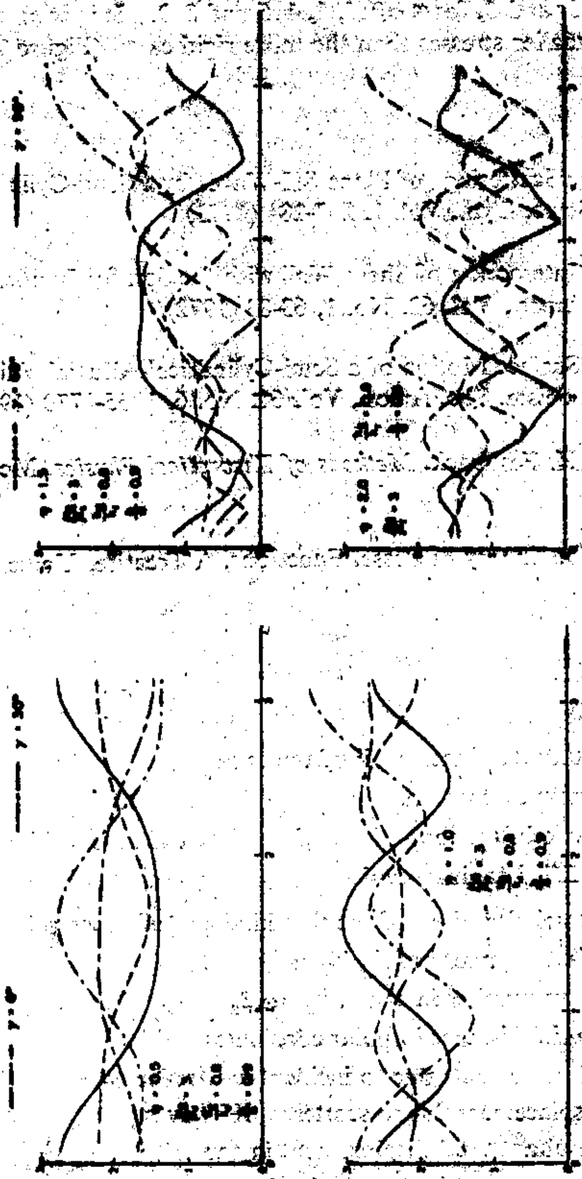

Figure 6 Normalized Stress Amplitudes for Incident SH Waves (γ=30°, 60°, 30°, 0° and [illegible])

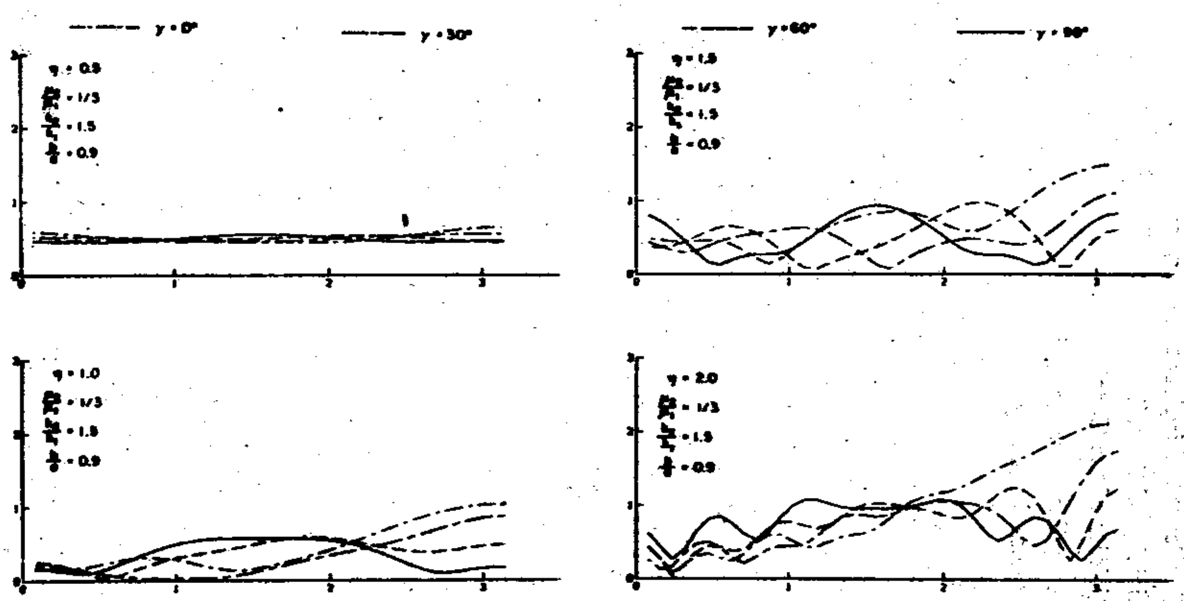

Figure 7 Normalized Stress Amplitudes for Incident SH Waves
(γ=90°, 60°, 30°, 0° and μ_2/μ_1=1/3, k_2/k_1=1.5, b/a=0.9)

η	Ratio of diameter of canal, 2a and λ, the wavelength of incident SH waves
θ	Azimuth in polar coordinates
λ	Wavelength of incident SH waves
μ_1	Rigidity of the soil
μ_2	Rigidity of the Canal
σ^*	Normalized stress amplitude
ω	Angular frequency